

This article was downloaded by:

On: 24 January 2011

Access details: *Access Details: Free Access*

Publisher *Taylor & Francis*

Informa Ltd Registered in England and Wales Registered Number: 1072954 Registered office: Mortimer House, 37-41 Mortimer Street, London W1T 3JH, UK



## Journal of Macromolecular Science, Part A

Publication details, including instructions for authors and subscription information:

<http://www.informaworld.com/smpp/title~content=t713597274>

### Reactions of Hydrated Electron with *N,N*-Methylenebisacrylamide in Aqueous Solution: A Pulse Radiolysis Study

M. S. Panajkar<sup>a</sup>; S. N. Guha<sup>a</sup>; C. Gopinathan<sup>a</sup>

<sup>a</sup> Chemistry Division, Bhabha Atomic Research Centre, Bombay, India

**To cite this Article** Panajkar, M. S. , Guha, S. N. and Gopinathan, C.(1995) 'Reactions of Hydrated Electron with *N,N*-Methylenebisacrylamide in Aqueous Solution: A Pulse Radiolysis Study', *Journal of Macromolecular Science, Part A*, 32: 1, 143 – 156

**To link to this Article:** DOI: 10.1080/10601329508011070

**URL:** <http://dx.doi.org/10.1080/10601329508011070>

PLEASE SCROLL DOWN FOR ARTICLE

Full terms and conditions of use: <http://www.informaworld.com/terms-and-conditions-of-access.pdf>

This article may be used for research, teaching and private study purposes. Any substantial or systematic reproduction, re-distribution, re-selling, loan or sub-licensing, systematic supply or distribution in any form to anyone is expressly forbidden.

The publisher does not give any warranty express or implied or make any representation that the contents will be complete or accurate or up to date. The accuracy of any instructions, formulae and drug doses should be independently verified with primary sources. The publisher shall not be liable for any loss, actions, claims, proceedings, demand or costs or damages whatsoever or howsoever caused arising directly or indirectly in connection with or arising out of the use of this material.

## REACTIONS OF HYDRATED ELECTRON WITH *N,N'*-METHYLENEBISACRYLAMIDE IN AQUEOUS SOLUTION: A PULSE RADIOLYSIS STUDY

M. S. PANAJKAR, S. N. GUHA, and C. GOPINATHAN

Chemistry Division  
Bhabha Atomic Research Centre  
Bombay 400085, India

### ABSTRACT

A hydrated electron reaction with *N,N'*-methylenebisacrylamide (MBA, M) was studied in aqueous solution at different pHs using the nanosecond pulse radiolysis technique. The rate constant for this reaction was very high ( $2.8 \pm 0.3 \times 10^{10} \text{ dm}^3 \cdot \text{mol}^{-1} \cdot \text{s}^{-1}$ ) and diffusion controlled. Transient  $M^{\cdot -}$  formed in the reaction of  $e_{\text{aq}}^-$  with MBA (M) were characterized by their absorption spectrum ( $\lambda_{\text{max}}$  at 290 and 380 nm), decay kinetics, and  $\text{p}K_a$ . The subsequent reaction immediately after electron addition was shown to be cyclization of the  $M^{\cdot -}$  species. The process of cyclization depends strongly on the pH of the medium and is faster as the pH is increased. Polymer formation was observed in the overall reaction, and evidence of the first propagation step leading to polymerization was provided.

### INTRODUCTION

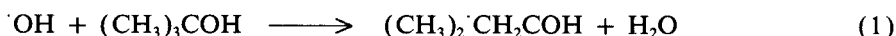
*N,N'*-Methylenebisacrylamide (MBA), a well-known bifunctional monomer, is mostly used as a crosslinking agent in polymer reactions, as a vulcanization agent for urethane rubbers, in finishes in the textile industry for improved surface properties, in compositions for the encapsulation of microorganisms, and as a flocculating agent in wastewater treatment. Studies of the homopolymerization of the monomer have been carried out using redox initiators [1–4] and the photosensitized

method [5]. The mechanism of polymerization in these reactions has been suggested to be free radical involving a cyclized species [5–9], but no direct evidence of the transients involved in the initial reactions has been provided. These studies have dealt mainly with the steady-state where the reaction mechanism for chemical polymerization has been based on final product analysis. Relatively little information is available about the exact nature of the intermediate species involved in the initiation and propagation steps leading to polymerization. Our aim for this work was to understand the nature of the initiating and propagating species involved in the hydrated electron ( $e_{\text{aq}}^-$ ) induced polymerization of MBA. This was achieved by analysis of the time-resolved spectrum of the transients produced in the pulse radiolysis of MBA. While the formation kinetics of the electron adduct of MBA has provided direct evidence of very high reactivity of  $e_{\text{aq}}^-$  with MBA, analysis of the decay of this species could supply evidence for cyclization of the adduct species leading to polymerization. Our study of the pH effect revealed the involvement of an acid–base equilibrium from which a  $\text{p}K_{\text{a}}$  of the adduct species was evaluated. From the kinetics of the different protolytic forms, it was possible to show which of the forms favors cyclization.

## EXPERIMENTAL

All chemicals used were GR grade. MBA from Sigma Chemicals was further purified by recrystallization from hot methyl alcohol at 50°C. Solutions were prepared in nanopure water having a conductivity of  $0.1 \mu\text{S}\cdot\text{cm}^{-1}$ , obtained by passing distilled water through a Barnsted Nanopure water system to remove all ionic and organic impurities. The reaction of  $e_{\text{aq}}^-$  was studied over the pH range of 4 to 12 and that of the H atom at pH  $\sim 2$ . The pH of the solution under investigation was adjusted using  $\text{H}_2\text{SO}_4$ ,  $\text{Na}_2\text{HPO}_4$ ,  $\text{KH}_2\text{PO}_4$ ,  $\text{Na}_2\text{B}_4\text{O}_7\cdot 10\text{H}_2\text{O}$ , and  $\text{NaOH}$  in suitable combinations. The concentrations of these buffer reagents were so adjusted that they did not interfere with the main reactions. A typical buffer concentration generally employed was  $5 \times 10^{-3} \text{ mol}\cdot\text{dm}^{-3}$ . Gases for purging the solutions were IOLAR grade from Indian Oxygen Ltd.

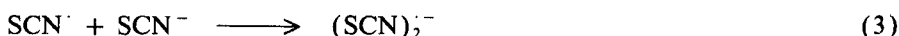
Pulse radiolysis of aqueous solution leads to the formation of  $e_{\text{aq}}^-$ ,  $\text{H}\cdot$ , and  $\text{OH}\cdot$  as the primary reactive species. The reactions of  $e_{\text{aq}}^-$  with MBA was studied in an  $\text{N}_2$ -saturated solution containing MBA and *t*-butanol in the pH range of 4 to 12. *t*-Butanol served as a scavenger of  $\text{OH}\cdot$  radicals, giving rise to unreactive  $(\text{CH}_3)_2\text{CH}_2\text{COH}$ :



H atoms are quantitatively converted to  $e_{\text{aq}}^-$  at pH  $> 4$ . Thus, the pulse radiolysis of the above matrix was used exclusively for studying the reaction of the hydrated electron. Details of the pulse radiolysis setup are given elsewhere [10]. For pulse radiolysis experiments, pulses of 7 MeV electrons of 50 nsec width were generally employed. For recording spectra, 2  $\mu\text{sec}$  pulses of 7 MeV electrons were employed; for kinetic studies, 50 nsec pulses were used.

In order to evaluate various parameters such as the extinction coefficient ( $\epsilon$ ), the rate constant for a chemical reaction, etc., it is necessary to know the concentration of the radical species generated. For this purpose, the dose per pulse absorbed

by a chemical system has to be determined. To measure the electron pulse dose, the well-known thiocyanate dosimeter was employed. An aerated aqueous solution of potassium thiocyanate (KSCN) ( $0.05 \text{ mol} \cdot \text{dm}^{-3}$ ) was exposed to the electron pulse. The OH radicals formed in water radiolysis oxidize thiocyanate ions ( $\text{SCN}^-$ ) via Eqs. (2) and (3) to give  $(\text{SCN})_2^-$  species having a characteristic visible absorption band.



$G\epsilon$  for  $(\text{SCN})_2^-$  is reported to be  $21,522 \text{ dm}^3 \cdot \text{mol}^{-1} \cdot \text{cm}^{-1}$  per 100 eV at 500 nm [11], where  $G$  is radiation chemical yield expressed as the number of molecules formed or destroyed per 100 eV of energy absorbed and  $\epsilon$  is the molar extinction coefficient of the  $(\text{SCN})_2^-$  radical. From the measured O.D. values, the dose absorbed per pulse is then computed by using the following expression:

$$\text{Dose absorbed} = \frac{\text{O.D.}}{G\epsilon} \frac{N}{1000} 100 \text{ eV} \cdot \text{cm}^{-3} \quad (4)$$

where  $N$  is Avogadro's number. By substituting values for  $G$  and the extinction coefficient  $\epsilon$ , the above expression can be written in the simplified form as

$$\text{Dose absorbed} = \text{O.D.} \times 2.8 \times 10^{18} \text{ eV} \cdot \text{cm}^{-3} \quad (5)$$

Generally, the electron pulse doses employed were of the order of about 16 Gy per pulse. However, for the estimation of the extinction coefficient, the formation rate constant, etc., a lower dose of about 7 Gy was employed. The extinction coefficient of the product transient species was evaluated at a desired wavelength ( $\lambda$ ) employing corrections for the ground state absorption by using the following relationship:

$$\epsilon_T = \epsilon_p + \frac{[(\text{O.D.})_T][G_{(\text{SCN})_2^-}][\epsilon_{(\text{SCN})_2^-}]}{G_T[(\text{O.D.})_{(\text{SCN})_2^-}]} \quad (6)$$

where  $\epsilon_p$  is the extinction coefficient in  $\text{dm}^3 \cdot \text{mol}^{-1} \cdot \text{cm}^{-1}$  of the parent molecule at wavelength  $\lambda$ ,  $G_T$  is the  $G$  value of the product transient species, and  $[(\text{O.D.})_T]$  and  $[(\text{O.D.})_{(\text{SCN})_2^-}]$  are the observed absorbances of the transient at  $\lambda$  and of the thiocyanate radical  $(\text{SCN})_2^-$  at 500 nm, respectively, under isodose condition.

## RESULTS AND DISCUSSION

### I. Reaction of Hydrated Electron with MBA

The hydrated electron signal monitored in an  $\text{O}_2$ -free *t*-butanol matrix at 720 nm was found to decay much faster in the presence of MBA than in its absence (Fig. 1a). This indicates high reactivity of this compound with  $e_{\text{aq}}^-$ . The rate constant for the reaction of  $e_{\text{aq}}^-$  with MBA was determined by following the decay of the hydrated electron at its  $\lambda_{\text{max}}$ , 720 nm, and also by directly monitoring the formation of the transient product generated as a result of this reaction. The formation kinetics of the electron adduct are discussed later in Section I.3.

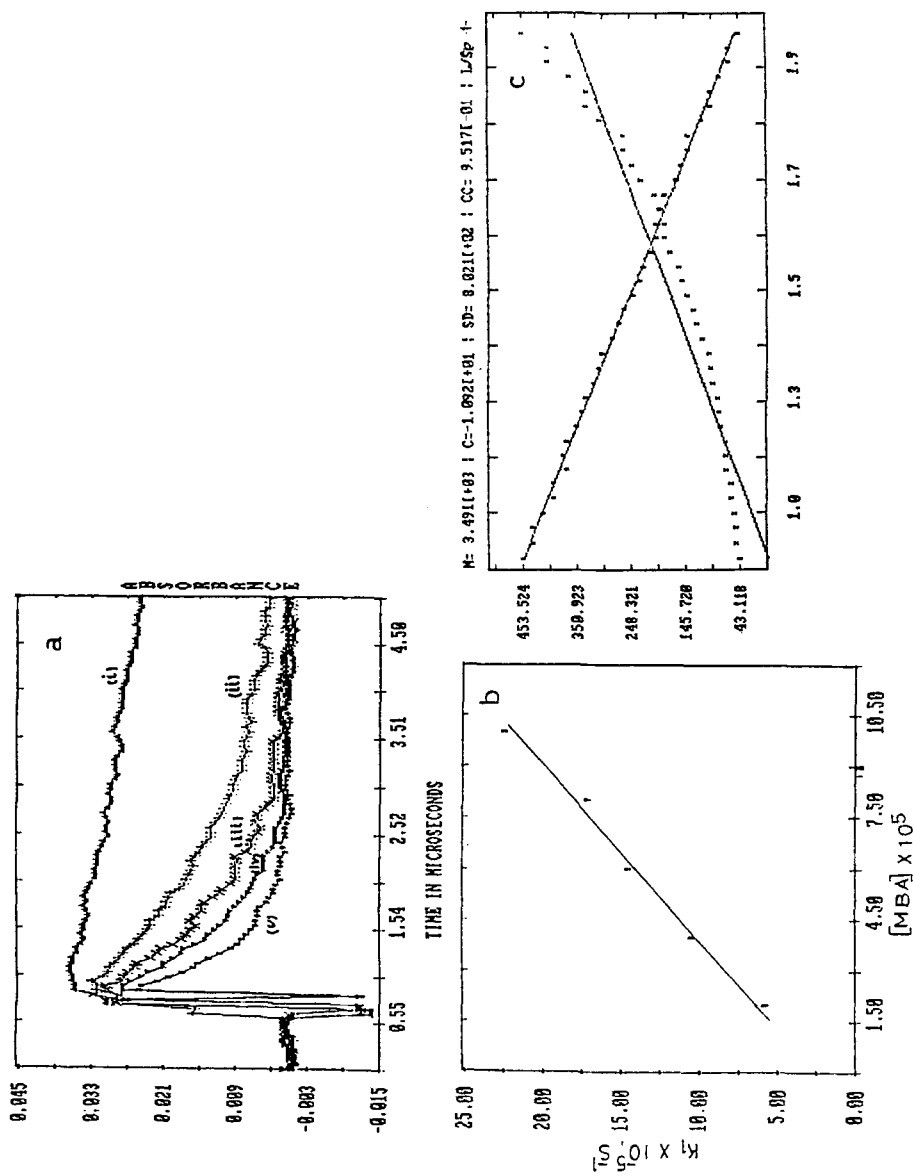


FIG. 1. (a) Decay of  $\epsilon_{eq}$  absorbance (720 nm) monitored at pH 7 in  $0.2 \text{ mol} \cdot \text{dm}^{-3}$  *t*-butanol matrix containing different concentrations of MBA: (i)  $0.0$ , (ii)  $1 \times 10^{-4}$ , (iii)  $2 \times 10^{-4}$ , (iv)  $4 \times 10^{-4}$ , and (v)  $6 \times 10^{-4} \text{ mol} \cdot \text{dm}^{-3}$ . (b) A plot of pseudofirst-order rate constant vs MBA concentration. (c) First- and second-order fit of decay kinetics.

### 1.1. Decay of $e_{\text{aq}}^-$

The decay of  $e_{\text{aq}}^-$  absorbance at pH 7 in the presence of MBA followed pseudo-first-order kinetics and depended on MBA concentration. A plot of pseudo-first-order rate constant vs MBA concentration was linear (Fig. 1b) and the bimolecular rate constant for the reaction of  $e_{\text{aq}}^-$  with MBA evaluated from this plot was found to be  $2.8 \pm 0.3 \times 10^{10} \text{ dm}^3 \cdot \text{mol}^{-1} \cdot \text{s}^{-1}$ . Reaction of a hydrated electron with MBA (M), leading to the generation of electron adduct,  $M^-$ , can be represented by



As we shall see in Section II, the  $e$ -adduct formed in the above reaction has a  $\text{p}K_{\text{a}}$  of 6.7 and hence the adduct is expected to exist as the anion radical,  $M'^-$ , at  $\text{pH} > 6.7$ , whereas below this pH the predominant form is neutral protonated MH radicals (Eq. 8, Section II).

### 1.2. Transient, $M^-$ Spectra

Time-resolved absorption spectra of the transient formed by the reaction of  $e_{\text{aq}}^-$  with MBA in an electron-beam pulsed  $\text{N}_2$ -saturated  $t$ -butanol ( $0.2 \text{ mol} \cdot \text{dm}^{-3}$ ) matrix containing  $5 \times 10^{-4} \text{ mol} \cdot \text{dm}^{-3}$  of MBA at pH 8.5 are shown in Fig. 2. At this pH the predominant form of the  $e$ -adduct would be the anion radical  $M'^-$ . A well-defined spectrum having an intense absorption band with  $\lambda_{\text{max}}$  at 290 nm ( $\epsilon = 9800 \text{ dm}^3 \cdot \text{mol}^{-1} \cdot \text{cm}^{-1}$ ) and a weak band with  $\lambda_{\text{max}}$  380 nm ( $\epsilon = 2500 \text{ dm}^3 \cdot \text{mol}^{-1} \cdot \text{cm}^{-1}$ ).

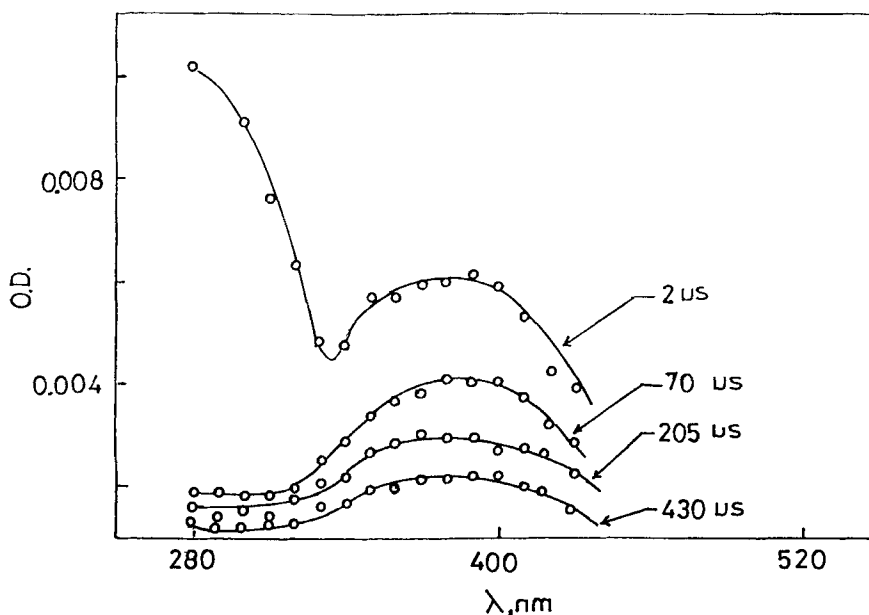


FIG. 2. Time resolved spectra of transients formed by hydrated electron reaction with MBA at pH 8.5 (matrix:  $[\text{MBA}] = 5 \times 10^{-4} \text{ mol} \cdot \text{dm}^{-3}$ ,  $[t\text{-butanol}] = 0.2 \text{ mol} \cdot \text{dm}^{-3}$ ,  $\text{O}_2$ -saturated system).

$\text{mol}^{-1}\cdot\text{cm}^{-1}$ ) can be seen in this time scale. It is observed that both the bands appear almost together immediately after the electron pulse, and the absorbances at these wavelengths decay simultaneously up to about  $70\ \mu\text{s}$ . Thereafter, the absorbances of these bands decayed very slowly, disappearing almost completely in  $\sim 1$  ms. It is inferred that the initial fast decaying species and the species subsequently formed, which decay in a longer time scale, have the same absorption bands with  $\lambda_{\text{max}}$  290 and 380 nm.

In the pulse radiolysis of acrylamide, Chambers et al. [12] reported the absorption spectrum of the transients formed in the overall reactions, which had bands with  $\lambda_{\text{max}}$  at 275 and 370 nm. These authors assigned the 275 nm band to the electron adduct and the 370 nm band to H and the OH adduct. On the basis of scavenger studies, it was later clarified [13] that  $\lambda_{\text{max}}$  290 nm is entirely due to the electron adduct and that this species has a second absorption maximum at 380 nm. They also confirmed that OH, and presumably the H adduct, also exhibit a band at 370 nm. Madhavan et al. [14] studied the hydrated electron reaction with this compound in *t*-butanol matrix at alkaline pH and reported 270 and 375 nm bands for the electron adduct of acrylamide. In the MBA molecule, two acrylamides are attached to a methylene group and it is expected to have a similar chromophore on addition of an electron to this molecule. On this line of thinking, our spectral observations for the electron adduct of MBA having bands at 290 and 380 nm appear to be quite genuine. The most probable site of electron addition is expected to be the carbonyl group C=O in the MBA molecule (see Section II.1 for a discussion).

### 1.3. Formation Kinetics of $e^-$ -Adduct, $M^{\cdot-}$

Oscilloscope traces recorded in an electron-beam pulsed  $\text{N}_2$ -saturated *t*-butanol matrix of pH  $\sim 7$  on a sensitive time scale show the build-up of absorbances at 290 and 380 nm and decay at 550 nm (Fig. 3). It should be noted that the absorbance at 550 nm is entirely due to  $e_{\text{aq}}^-$ . When we consider the traces recorded at 290 and 550 nm, it is observed that the build-up of absorbance at 290 nm after the electron pulse occurred over the same time period ( $\sim 2\ \mu\text{s}$ ) as that of the decay of absorbance at 550 nm. This also confirms that hydrated electron reacts with MBA and can be represented by Eq. (7).

In the absorption trace of 380 nm (Fig. 3b), the build-up of absorbance is seen to occur almost immediately after the electron pulse. Our time-resolved study indicated that the 290 and 380 nm absorption bands are due to one species,  $M^{\cdot-}$ , which, as stated before, exists as an anion radical at higher pH. The prompt build-up of 380 nm absorption can possibly be due to interference by the small absorbance of  $e_{\text{aq}}^-$  occurring at this wavelength with that of the transient  $M^{\cdot-}$  formed. From the nature of this trace (Fig. 3b), it appears that the extinction coefficients of the electron adduct,  $M^{\cdot-}$ , and the hydrated electron at 380 nm are very close to each other. On the other hand, absorption due to  $e_{\text{aq}}^-$  at 290 nm is negligibly small compared to that of the  $M^{\cdot-}$  species, and therefore the formation of  $M^{\cdot-}$  as monitored at 290 nm was free from such interference. In view of this, we considered only the 290 nm band of  $M^{\cdot-}$  for the study of formation kinetics.

The absorbance traces of 290 nm analyzed for different concentrations of MBA indicated that the build-up of these absorbances was pseudo-first-order with respect to MBA concentration. The bimolecular rate constant for the reaction of  $e_{\text{aq}}^-$  with MBA evaluated from the pseudo-first-order kinetics was  $2.7 \pm 0.5 \times 10^{10}\ \text{mol}^{-1}\cdot\text{dm}^3\cdot\text{s}^{-1}$ . Although the uncertainty in the determination is quite high, this

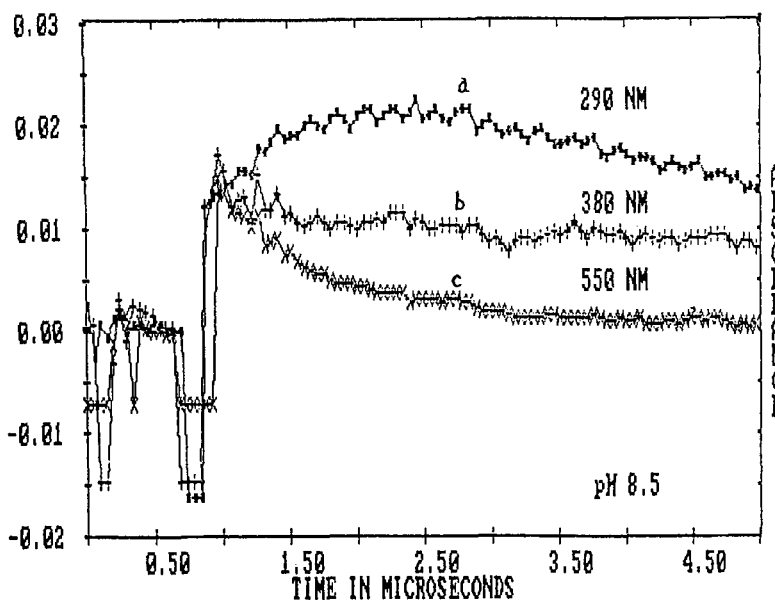


FIG. 3. Oscilloscope traces recorded at 290, 380, and 550 nm in  $N_2$ -saturated *t*-butanol ( $0.2 \text{ mol} \cdot \text{dm}^{-3}$ ) matrix containing  $5 \times 10^{-4} \text{ mol} \cdot \text{dm}^{-3}$  MBA at pH 7.

value is within experimental error and is close to the one determined by following  $e_{\text{aq}}^-$  decay (Section I.1). Thus, these results demonstrate that the hydrated electron reacts with monomer M at an almost diffusion-controlled rate to give an electron adduct which has a prominent absorption band with  $\lambda_{\text{max}}$  290 nm and a weak band with  $\lambda_{\text{max}}$  380 nm.

## II. $pK_a$ of the Electron Adduct

Transient spectra recorded at pH 5 and 8.5 in an electron-beam pulsed  $N_2$ -saturated solution containing  $4 \times 10^{-3} \text{ mol} \cdot \text{dm}^{-3}$  of MBA and  $0.4 \text{ mol} \cdot \text{dm}^{-3}$  *t*-butanol are shown in Fig. 4. Both the spectra reveal two prominent absorption bands. However, the bands observed at pH 5 are blue shifted by  $\sim 10 \text{ nm}$  and the absorbances measured at a given wavelength are somewhat different as compared to those observed at pH 8.5 under isodose conditions. The radiation chemical yield for the hydrated electron does not differ enough in this pH range to account for such a difference in the absorbances. The pH effect can be attributed to the involvement of an acid-base equilibrium. It should be noted that the radiation chemical yield for the H-atom,  $G(\text{H})$ , is 0.55 in this pH range as against 2.8 for  $G(e_{\text{aq}}^-)$ , and therefore the interference due to H-atom reaction is not significant in the pH range studied. Moreover, the spectrum of the transient formed exclusively by the reaction of H-atom at pH 2 in an electron-beam pulsed oxygen-free *t*-butanol matrix containing MBA did not reveal any UV band as was observed in the case of the electron adduct at higher pH. However, a weak band with  $\lambda_{\text{max}}$  390 nm, possibly due to the H-adduct, was observed at pH 2. Therefore, at higher pH a small interference [corresponding to  $G(\text{H}) = 0.55$ ] is expected at the longer wavelength band of the  $e$ -adduct. The effect of pH on the absorbance of the 290 nm band of the electron



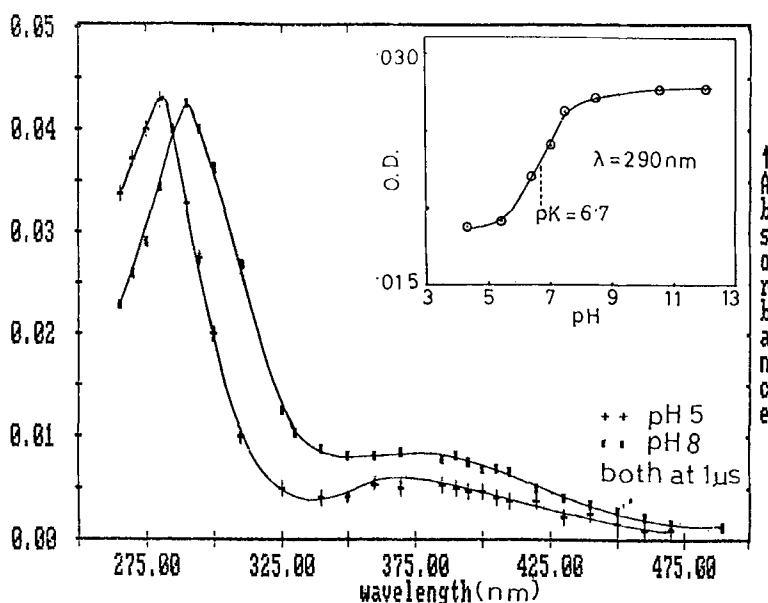


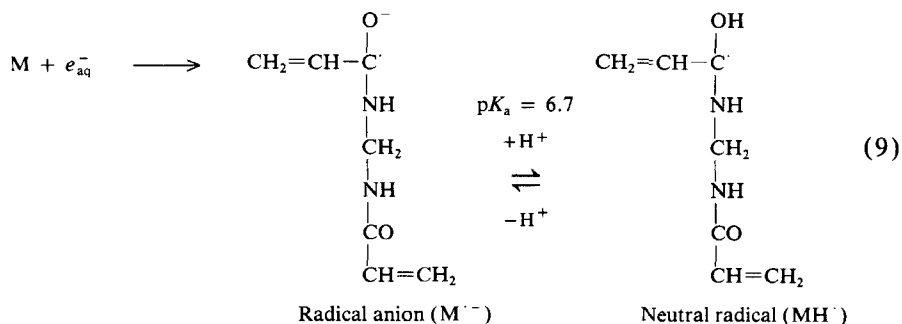
FIG. 4. Spectra of transients formed by hydrated electron reaction with MBA ( $4 \times 10^{-3} \text{ mol} \cdot \text{dm}^{-3}$ ) at pH 5 and 8.5 in  $\text{O}_2$ -free *t*-butanol ( $0.4 \text{ mol} \cdot \text{dm}^{-3}$ ) matrix. Inset: A typical  $\text{p}K_a$  curve of *e*-adduct of MBA: Variation of O.D. measured at 290 nm as a function of pH.

adduct over the pH 4 to 12 range was therefore studied. A typical  $\text{p}K_a$  curve (inset of Fig. 4) was obtained from which an inflection point at pH 6.7 corresponding to the  $\text{p}K_a$  of the electron adduct was inferred. The acid-base equilibrium of the transient can be represented by



Thus, the anion radical  $\text{M}^-$  undergoes protonation at  $\text{pH} < 6.7$  to give a neutral MH radical. The extinction coefficients of the anion and the neutral radical were estimated to be  $\epsilon_{290 \text{ nm}} = 9800$ ;  $\epsilon_{380 \text{ nm}} = 2500$  and  $\epsilon_{280 \text{ nm}} = 9890$ ;  $\epsilon_{370 \text{ nm}} = 1780 \text{ dm}^3 \cdot \text{mol}^{-1} \cdot \text{cm}^{-1}$  at their respective  $\lambda_{\text{max}}$  positions.

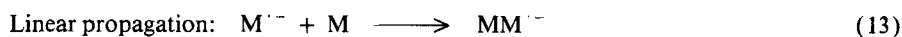
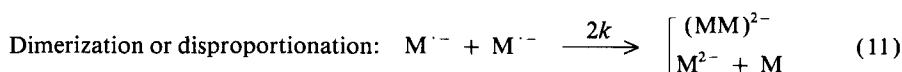
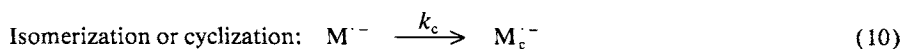
In the MBA molecule, because the carbonyl group is electron deficient, it is the most probable site of attack (see Section II.1) for the electron [15]. In view of our observed  $\text{p}K_a$  of 6.7, the structures shown in Eq. (9) could be assigned to the two conjugate acid-base forms of the transient adduct species:



### II.1. Decay Kinetics of the *e*-Adduct at Different pHs

As mentioned in Section I.2, the decay of absorbances at 290 and 380 nm as monitored at neutral pH consists of two components, one due to a fast and one due to a slowly decaying transient species. As far as the initial decay is concerned, it was observed that the decay of absorbances of the 290 and 380 nm bands followed good first-order kinetics (up to about 70  $\mu\text{s}$ ) and the rate constants were independent of parent MBA concentration, at least up to about  $9 \times 10^{-3} \text{ mol}\cdot\text{dm}^{-3}$ , the highest possible concentration employed for the experiment. Concentrations higher than this were found to cause turbidity on exposure to an electron pulse. The first-order rate constant values obtained by analysis of the decay of the initial absorbance at the two bands were close to each other. This also supports the idea that the transient bands at 290 and 380 nm are due to one and the same species formed by the reaction of  $e_{\text{aq}}^-$  with MBA. Since at pH 7 and above the predominant form of the *e*-adduct is the deprotonated  $M^{\cdot-}$ , the above kinetic behavior can be assigned to this anion radical. As mentioned above, the decay of the absorbances at 290 and 380 nm assigned to the electron adduct,  $M^{\cdot-}$ , at pH above 7 followed first-order kinetics (up to  $\sim 70 \mu\text{s}$ ), and the rate of decay was not dependent on the parent MBA concentration. During the initial stages of the experiment, it was found that the decay was becoming considerably faster when oxygen was introduced in the matrix. Utmost care was therefore taken to eliminate oxygen from the system. Hence, the first-order decay cannot be attributed to contamination of oxygen in the matrix. The effects of the variation of other parameters, such as buffer, ionic strength, and pH, were also studied. Among these parameters, only the pH of the system was found to affect the decay kinetics. Thus, the first-order rate constant, which was found to be  $0.9 \pm 0.3 \times 10^4 \text{ s}^{-1}$  at pH 4.8, increased to a value of  $2 \pm 0.3 \times 10^5 \text{ s}^{-1}$  almost an order of magnitude higher at pH 8. It is apparent that the first-order decay process is facilitated in the case of the deprotonated form  $M^{\cdot-}$  and is not favored at lower pH where the transient species exist as neutral MH radical. The pH study thus indicates the anion radical  $M^{\cdot-}$  to be the most active species.

The various pathways by which this anionic radical could decay can be represented by Processes (10)–(13) of Scheme 1, where HB denotes the buffer molecule ( $\text{Na}_2\text{HPO}_4$ ,  $\text{KH}_2\text{PO}_4$ , etc.) employed in this work.

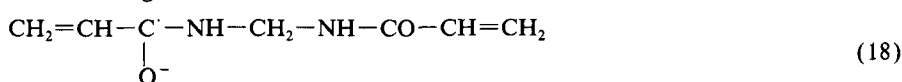
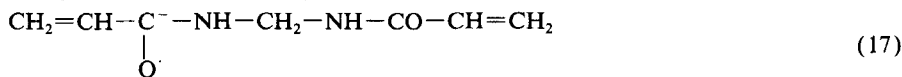
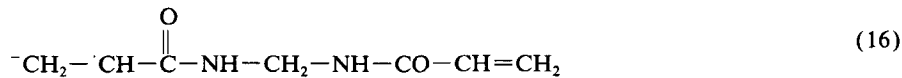
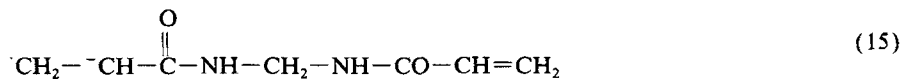
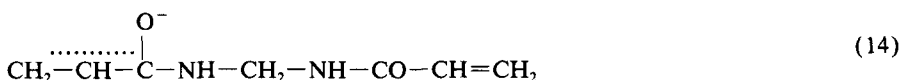


#### SCHEME 1.

Decay of the anion radical ( $M^{\cdot-}$ ), which followed very good first-order kinetics, did not change to second order even at twice the radical concentration (at higher dose). Hence, the process of dimerization or disproportionation (Eq. 11) is ruled out. The acid-catalyzed reaction (Eq. 12) or the propagation step (Eq. 13) also do

not seem to be feasible since an increase in buffer concentration to about 10-fold (from 2 to 20 mM) or monomer concentration (from 1 to 9 mM) could not affect the decay kinetics. We therefore assume that the step represented by Eq. (10), cyclization or isomerization, is the most likely process by which  $M^{\cdot -}$  disappears. From structural considerations, isomerization of long linear molecule can be ruled out, leaving only the option of cyclization.

In the case of chemically initiated polymerization of this monomer, Ratnasabhapathy et al. [6] proposed cyclization of the monomer radical formed by  $SO_4^{\cdot -}$  in the initial step, although there was no direct evidence of cyclization provided in their steady-state work. A similar mechanism has also been proposed by other workers [5, 7]. In steady-state gamma radiolysis of  $N_2$ -saturated MBA solution in a *t*-butanol matrix, we observed white colored turbidity due to the formation of its polymer. A similar observation was made for such a matrix when it was exposed to repeated electron pulses. Our observation of pure first-order decay could possibly be explained on the basis of a similar cyclization occurring immediately after the initial formation of the electron adduct  $M^{\cdot -}$  (the rate constant for the cyclization at  $pH > 6.7$  is  $2 \pm 0.3 \times 10^5 s^{-1}$ ), various canonical forms of which can be represented as shown in Scheme 2.



SCHEME 2.

In a pulse radiolysis study of acrylamide [12], out of the various canonical forms of the electron adduct of acrylamide ( $CH_2=CH-CO-NH_2$ ), the allylic type of radical form  $CH_2-\dot{C}H-CO-NH_2$  was shown to be responsible for the bands at 280 and 390 nm. In the MBA molecule, since the carbonyl group  $C=O$  is more electron deficient than the  $C=C$  group, an electron would add initially to the former, and in analogy to acrylamide, the allylic radical represented by Structure 14 in Scheme 2 could be the most probable structure of the electron adduct.

Subsequent to the decay of  $M^{\cdot -}$ , a corresponding build-up of absorption due to the cyclized species was observed at 290 nm. The decay traces of  $M^{\cdot -}$  recorded at 290 and 380 nm show two distinct portions (Fig. 5) which decay at two different rates. The first part, which decays very fast, can be ascribed to  $M^{\cdot -}$  whereas there is subsequent slower decay to the cyclized species  $M_c^{\cdot -}$ . As mentioned before, the secondary radical formed subsequent to the decay of  $M^{\cdot -}$  has absorption bands with  $\lambda_{max}$  290 and 380 nm and is identified as the cyclized  $M_c^{\cdot -}$  species. Since the

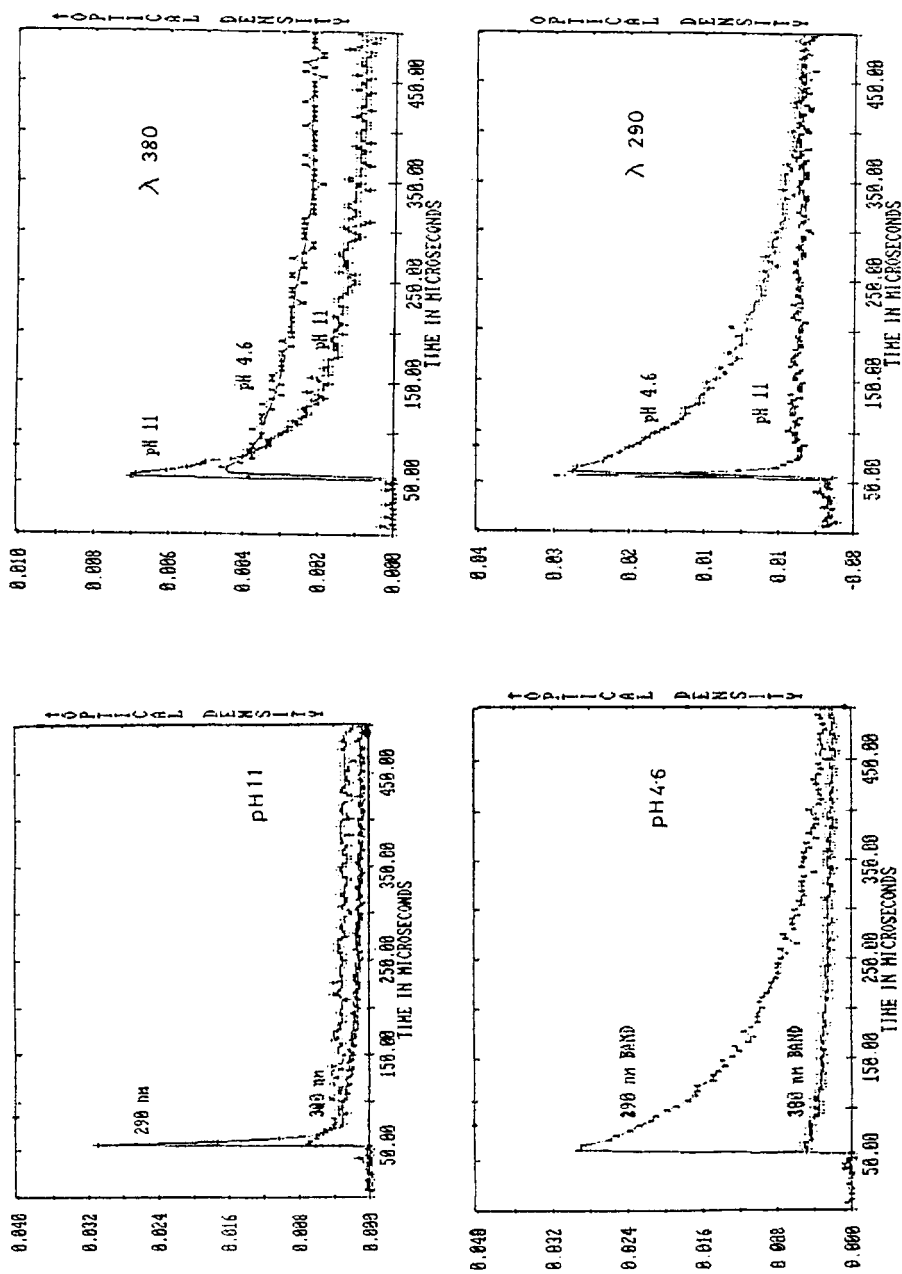
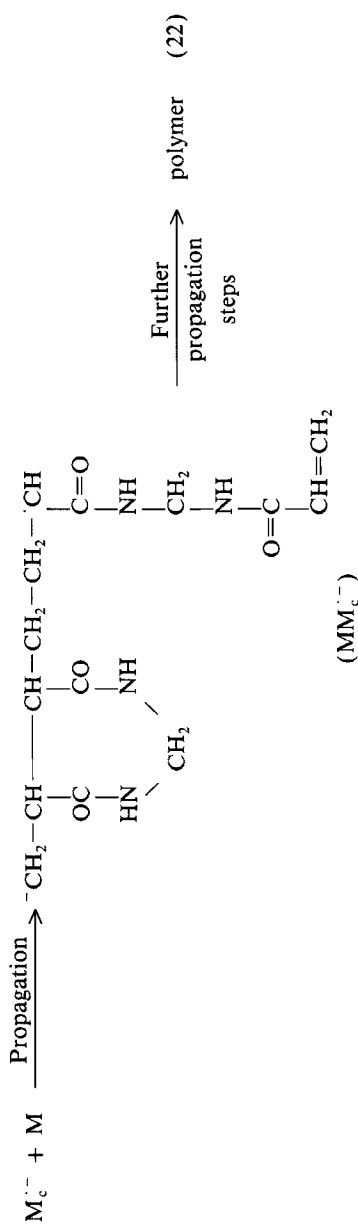
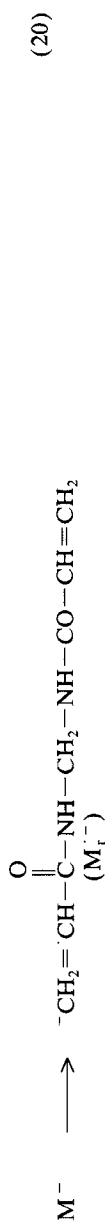
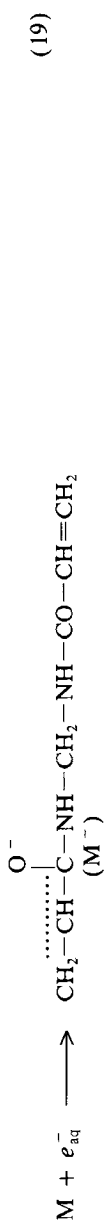


FIG. 5. Typical decay traces of the  $e^-$ -adduct formed by  $e^-_{aq}$  reaction in an electron pulsed  $N_2$ -saturated  $1 \times 10^{-3}$  mol  $\cdot$  dm $^{-3}$  MBA containing  $0.3$  mol  $\cdot$  dm $^{-3}$  *t*-butanol.



SCHEME 3.

absorbance of the cyclized species at 290 nm is considerably lower, we monitored the decay at 380 nm on a longer time scale in the presence of varying concentrations of MBA. Because this band has interference from the absorption of the primary M species, it was not possible to do a quantitative analysis. However, a rough estimate of the order of  $6 \pm 0.5 \times 10^6 \text{ dm}^3 \cdot \text{mol}^{-1} \cdot \text{s}^{-1}$  can be given for the reaction  $M_c^- + M \rightarrow MM_c^-$ , which represents the first propagation step. On the basis of these results, it is therefore proposed that the transient formed by the reaction of  $e_{\text{aq}}^-$  with MBA undergoes cyclization (Eq. 10, Scheme 1) in the initial period. This is in agreement with the earlier studies of MBA polymerization using chemical initiators, where a radical mechanism has been proposed involving cyclized radical species [5–7]. For the allylic form of  $M^-$  (Structure 14, Scheme 2) to cyclize (Eq. 21), the electron-hopping mechanism of Scheme 3 (Eq. 20) is proposed followed by a propagation step (Eq. 22) finally leading to the formation of an insoluble polymer.

Although the possibility of an 8-membered ring can also be considered by analogy to the conclusion of Matsumoto et al. [16] on acrylic anhydride cyclopolymerization, a 7-membered ring (see the structure in Eq. 21) would be more favored from steric and electrostatic considerations in MBA polymerization. A partial linear dimer  $MM_c^-$  (Eq. 22, Scheme 3) radical could possibly further cyclize prior to the addition of another monomer molecule, since a linear build-up of the polymer molecule with subsequent addition of monomer molecules would be sterically hindered. This propagation step could not, however, be established. Subsequent propagation steps would increase the molecular weight of the polymer and lead to the formation of an insoluble polymer.

Thus, it appears that cyclization of the anionic radical formed is very fast, and this step cannot be bypassed in the process of polymerization. The competing process of linear propagation (represented by Eq. 13) could not be induced even at MBA concentration as high as 9 mM, thus corroborating the fact that linear monovinyl-type propagation is sterically hindered due to long pendant groups with double bonds [6]. The yield of polymer as the final product could possibly be controlled by adjustment of the pH of the system but this has to be done by actual experiment under steady-state conditions. Steady-state experiments are in progress to verify these points. Studies are being continued to understand the mechanism in this system by using OH as the primary reacting radical.

## CONCLUSION

The reactivity of MBA toward  $e_{\text{aq}}^-$  is very high, and the rate constant for this initiation reaction is close to the diffusion-controlled value. The electron adduct formed immediately after the  $e_{\text{aq}}^-$  reaction with the monomer has been shown to exist in two conjugate acid–base forms with  $\text{p}K_{\text{a}} = 6.7$ . These forms of the  $e$ -adduct exist predominantly as the anion and the neutral radical at pH above and below 6.7, respectively. The anion radical undergoes fast cyclization with a first-order rate constant of  $2 \pm 0.3 \times 10^5 \text{ s}^{-1}$ , whereas cyclization is less favored in the case of neutral species. The cyclized species decay with a bimolecular rate constant of  $6 \pm 0.5 \times 10^6 \text{ dm}^3 \cdot \text{mol}^{-1} \cdot \text{s}^{-1}$  is attributable to the first propagation step. It is concluded that the electron adduct (anion radical) undergoes cyclization prior to propagation, which finally leads to the formation of an insoluble polymer.

## ACKNOWLEDGMENT

The authors wish to thank Dr. J. P. Mittal, Associate Director, Chemistry Group, for his encouragement during the course of this work.

## REFERENCES

- [1] N. R. Subbaratnam, S. P. Manickam, P. Venuvanalingam, and A. Gopalam, *J. Macromol. Sci. — Chem.*, **A23**, 117 (1986).
- [2] A. Gopalan, P. Venuvanalingam, S. P. Manickam, K. Venkatrao, and N. R. Subbaratnam, *Eur. Polym. J.*, **18**, 531 (1982).
- [3] S. Paulrajan, A. Gopalan, K. Venkatrao, and N. R. Subbaratnam, *Polymer*, **24**, 906 (1983).
- [4] T. Parthasarathy, K. Nageswar Rao, B. Sethuram, and T. Navaneeth Rao, *J. Polym. Mater.*, **3**, 191 (1986).
- [5] B. Suresh Babu, K. Nageswar Rao, B. Sethuram, and T. Navaneeth Rao, *J. Macromol. Sci. — Chem.*, **A25**(1), 109 (1988).
- [6] S. Ratnasabapathy, N. Mariasami, and S. P. Manickam, *Ibid.*, **A25**(1), 83 (1988).
- [7] S. Ratnasabapathy, N. Mariasami, S. P. Manickam, K. Venkatrao, and N. R. Subbaratnam, *Ibid.*, **A25**(1), 97 (1988).
- [8] R. Das, K. Behari, and U. Agrawal, *J. Polym. Sci., Polym. Chem. Ed.*, **31**, 1449 (1993).
- [9] R. Das, K. Behari, and U. Agrawal, *Polym. Int.*, **31**, 235 (1993).
- [10] S. N. Guha, P. N. Moorthy, K. Kishore, D. B. Naik, and K. N. Rao, *Proc. Indian Acad. Sci. (Chem. Sci.)*, **99**, 261 (1987).
- [11] E. M. Fielden, "Chemical Dosimetry of Pulsed Electron and X-Ray Sources in the 1–20 MeV Range," in *The Study of Fast Processes and Transient Species by Electron Pulse Radiolysis* (J. H. Baxendale and F. Busi, Eds.), D. Reidel, Dordrecht, Holland, 1982, pp. 49–62.
- [12] K. W. Chambers, E. Collinson, F. S. Dainton, W. A. Seddon, and F. Wilkinson, *Trans. Faraday Soc.*, **63**, 1699 (1967).
- [13] K. W. Chambers, E. Collinson, and F. S. Dainton, *Ibid.*, **66**, 142 (1970).
- [14] V. Madhavan, N. N. Lichtin, and E. Hayon, *J. Am. Chem. Soc.*, **97**, 2989 (1975).
- [15] J. Lilie, G. Beck, and A. Henglein, *Ber. Bunsenges. Phys. Chem.*, **73**, 170 (1969).
- [16] A. Matsumoto, T. Kitamura, M. Oiwa, and G. B. Butler, *J. Polym. Sci., Polym. Chem. Ed.*, **19**, 2531 (1951).

Received August 3, 1993

Revision received April 18, 1994